BELLCOMM, INC.
955 L'ENFANT PLAZA NORTH, S.W. WASHINGTON, D.C. 20024

COVER SHEET FOR TECHNICAL MEMORANDUM

TITLE- On Space Vehicle Attitude Stabilization by Passive Control Moment Gyros

TM- 68-1022-9

DATE- November 8, 1968

FILING CASE NO(S)- 620

AUTHOR(S)- J. W. Schindelin

FILING SUBJECT(S)- (ASSIGNED BY AUTHOR(S)- Space Vehicle Attitude Stabilization
Passive Control Moment Gyros

ABSTRACT

In this paper the basic equations of motion for space vehicles with various passive CMG configurations are presented. As the exact equations of motion are nonlinear, linear models or linearized expressions have been established. This is of major importance especially for system design as the linearized equations allow one to determine explicitly the influence of system parameters on performance. It was found that for step and sinusoidal input functions, the errors due to linearization are less than 1%.

Special attention was given to friction phenomena, i.e., viscous and Coulomb friction, which arise in connection with the motion of the CMGs about their respective gimbal axes. It was found that friction decisively influences system performance. Coulomb friction, in general, severely restricts the attitude stabilization capability of the CMGs until the space vehicle has attained a certain angular velocity.

SEE REVERSE SIDE FOR DISTRIBUTION LIST

BELLCOMM, INC.

SUBJECT: On Space Vehicle Attitude Stabilization by Passive Control Moment Gyros Case 620

DATE: November 8, 1968

FROM: J. W. Schindelin

TM-68-1022-9

TECHNICAL MEMORANDUM

1.0 INTRODUCTION

It is of interest to inquire into attitude stabilization of space vehicles by passive Control Moment Gyros for possible use in the Apollo Applications Program.

A Control Moment Gyro (CMG) is basically a gimballed reaction wheel with, in general, two gimbals. In this arrangement, it is a 2-degree of freedom device if it is assumed that the angular velocity of the wheel stays constant. Otherwise, a third degree of freedom is obtained. Torquers at each gimbal provide that the orientation of the CMG's spin angular momentum vector can be changed with respect to a reference frame, i.e., a coordinate system which is fixed to the space vehicle. The passive CMG considered in this paper has one degree of freedom; one gimbal stays locked in a certain angular position. Secondly, the term passive is used to indicate that no external torque is applied on the CMG through the torquer of the free gimbal. Then the CMG moves about this gimbal axis only under the influence of torques which are due to coupling effects from the motion of the space vehicle.

In this paper the basic equations of motion for space vehicles with various CMG configurations are presented. As the exact equations of motion are nonlinear, linear models or linearized expressions have been established. This is of major importance especially for system design as the linearized equations allow one to determine explicitly the influence of system parameters on performance.

Special attention was given to friction which arises in connection with the motion of the CMGs about their respective gimbal axes. It was found that friction decisively influences system's performance.

Investigations on AAP-cluster stabilization by passive control moment gyros, the results of which are presented in [8], are based on this report.

2.0 DESCRIPTION OF THE SYSTEM

2.1 General Explanations

In its most general configuration the system which will be analyzed in this paper is composed of a rigid body, called the carrier, and of an arbitrary number of single degree of freedom Control Moment Gyros (CMGs) mounted within the carrier. However, in the paper, the detailed analysis is restricted to configurations with at most 3 CMGs. The so called SIXPAC CMG configuration, as is shown in Figure 1, represents one possible CMG arrangement [1]. These CMGs have basically 2 degrees of freedom, but by locking any one of the two gimbals of each CMG, single degree of freedom devices are obtained. If the particular gimbals are locked at certain angular positions, specific initial orientations of the spin angular momentum vectors of the CMGs can be arranged. It is important to select the initial orientations in such a way as to make the best use of the stabilization properties of the CMGs in the presence of the external torques that act on the carrier in its desired attitude.

The CMGs are designated by the index k, $(k=1,2,3)$, with the corresponding angular momentum vector $\vec{H}_k$ and the outer and inner gimbal angles α_k and β_k.

2.2 Coordinate Systems and System Vectors (See Figure 2)

For the analysis the following right hand Cartesian coordinate systems and vectors are introduced:

a. The inertially fixed $X^rY^rZ^r$ reference system.

b. A $X^bY^bZ^b$ coordinate system which is fixed to the carrier having its origin at the carrier's center of mass $(c.m.)_b$. This coordinate system rotates with respect to the inertial system with the angular velocity $\vec{\Omega}$. The system vector $\vec{Q}^k$ which is referred to this coordinate system goes from $(c.m.)_b$ to the center of mass $(c.m.)_k$, of the k^{th}-CMG.

c. The XYZ coordinate system with origin at the center of mass, c.m., of the total configuration (carrier and CMGs). The system vectors $\vec{R}^k$ and $\vec{P}$ which are referred to this coordinate system, go from c.m. to $(c.m.)_k$ and c.m. to $(c.m.)_b$, respectively. The respective XYZ and $X^bY^bZ^b$ coordinate axes shall always be parallel.

d. With its origin at the center of mass, $(c.m.)_k$, of the k^{th} - CMG there is a $X^kY^kZ^k$ coordinate system. It is assumed here that the $(c.m.)_k$ is identical with the center of mass of the CMG's flywheel. This coordinate system is fixed to the flywheel. It rotates with respect to the carrier with the angular velocity $\vec{\Omega}^k$. Also, the free gimbal of the CMG shall go through $(c.m.)_k$.

The orientation of the $X^kY^kZ^k$ coordinate system with respect to $X^bY^bZ^b$ is given by the transformation

$$\begin{pmatrix} X^k \\ Y^k \\ Z^k \end{pmatrix} = (A^k) \begin{pmatrix} X^b \\ Y^b \\ Z^b \end{pmatrix} \tag{1}$$

where (A^k) is, in general, a 3 x 3 matrix.

For the vector $\vec{P}$ the expression is obtained [2]

$$\vec{P} = - \frac{\sum_k M^k \vec{Q}^k}{M^b + \sum_k M^k} \tag{2}$$

where M^k is the mass of the k^{th}-CMG and M^b the mass of the carrier, respectively.

3.0 EQUATIONS OF MOTION. GENERAL EXPRESSIONS

3.1 Carrier

The angular momentum of the total configuration, carrier and CMGs, with respect to c.m. is given by the expression [2], Equation (20), $\dot{\vec{Q}}^k = 0$

$$\vec{L} = I^b \cdot \vec{\Omega} + \sum_k I^k \cdot \vec{\Omega}_g^k + \sum_k M^k \{\vec{R}^k \times (\vec{\Omega} \times \vec{Q}^k)\} \tag{3}$$

The vector

$$\vec{\Omega}_g^k = \vec{\Omega} + \vec{\Omega}^k \tag{4}$$

is the total angular velocity of this CMG with respect to inertial space. I^b is the inertia tensor of the carrier without the CMGs, referred to the $X^bY^bZ^b$ coordinate system, and I^k represents the inertia tensor of the flywheel of the k^{th}-CMG, referred to XYZ coordinates. The third term in (3) takes into consideration the locations of the CMGs within the carrier. Because, the last term is a linear function of the angular velocity $\vec{\Omega}$, one can add its components directly to the components of the first terms in (3), thus essentially changing the value of the elements of I^b. For the investigation in this paper, the third term in (3) will be neglected. Its influence is, generally, very small and, as has been just outlined, this term produces analytically no additional problems.

From Newton's law the equation for the carrier vehicle's attitude motion is given by the expression [3]

$$\vec{N} = \dot{\vec{L}} + \vec{\Omega} \times \vec{L} \tag{5}$$

with $\vec{N}$ as the vector of the external torque which acts on the carrier, the angular momentum vector $\vec{L}$ which is expressed in (3), and its rate of change with respect to time $\dot{\vec{L}}$. In order to evaluate (5) explicitly, the vectors have to be expressed in the $X^bY^bZ^b$ coordinate system.

The translational motion of the c.m. is given by the equation

$$\vec{F} = [M^b + \sum_k M^k] \frac{d}{dt}(\vec{V})$$

where $\vec{F}$ is the vector of the total external force which acts on this configuration and $\vec{V}$ is the translational velocity of the c.m. Since it is assumed that every CMG gimbal axis goes through the center of mass of the respective CMG, there is no coupling between the translational motion of c.m. and the attitude motions of the CMGs.

3.2 K^{th}-CMG

The total angular momentum $\vec{L}^k$ of the k^{th}-CMG with respect to $(c.m.)_k$ is

$$\vec{L}^k = I^k \cdot \vec{\Omega}_g^k \tag{6}$$

The equation of motion for this CMG is given by the expression [3]

$$\vec{N}^k = \dot{\vec{L}}^k + \vec{\Omega}_g^k \times \vec{L}^k + \text{friction terms} \tag{7}$$

where $\vec{N}^k$ is the external torque that acts on this CMG and $\dot{\vec{L}}^k$ is the time rate of change of the angular momentum $\vec{L}^k$. Because the stabilization of the carrier by passive CMGs is considered in this paper, all vectors $\vec{N}^k$ are zero. Here $\vec{N}^k$ is identical with the external torque which is provided by torquers. Any other external torques, e.g., a torque due to gravity gradient phenomenon, will be neglected. In addition to the inertial terms in (7), which are obtained by applying Newton's law to (6), frictional torques have to be taken into account. These arise from friction phenomena due to the motion about the CMG's gimbal. In order to evaluate (7) explicitly, all vectors have to be expressed in the $X^kY^kZ^k$ coordinate system. The components of the inertia terms must be resolved along the respective gimbal axes. The addition of the appropriate friction terms finally yields the total equation of motion. The friction terms considered in this paper are viscous friction and Coulomb friction. Both phenomena are treated as functions of gimbal angular velocity.

4.0 EXACT EQUATIONS OF MOTION FOR VARIOUS CMG CONFIGURATIONS

4.1 The 2-CMG Configuration

Figure 3 shows the vectors $\vec{H}_1$, $\dot{\vec{\alpha}}_1$, (k=1), and $\vec{H}_3$, $\dot{\vec{\beta}}_3$, (k=3) (spin angular momentum and gimbal angular velocity) of the two CMGs of this configuration. The selection of the CMGs and the orientation of their respective spin angular momentum and gimbal angular velocity vectors is such as to obtain for the carrier the best attitude stabilization properties with respect to external

torques about the vehicle's Z^b coordinate axis. Both spin angular momentum vectors can move in the X^bZ^b coordinate plane, and their respective gimbal angular velocity vectors are parallel to the Y^b axis.

4.11 Derivation of the Transformation (A^1)

According to (1) the transformation

$$\begin{pmatrix} X^1 \\ Y^1 \\ Z^1 \end{pmatrix} = (A^1) \begin{pmatrix} X^b \\ Y^b \\ Z^b \end{pmatrix} \tag{8}$$

gives the orientation of the $X^1Y^1Z^1$ coordinate system with respect to $X^bY^bZ^b$. According to Figure 4, (A^1) is obtained from two successive right hand rotations through the angle α_1, about the Y^b axis, and the angle π_1, about the X^1 axis, respectively. It is

$$(A^1) = (\pi^1)(\alpha^1) \tag{9}$$

where +)

$$(\alpha^1) = \begin{pmatrix} C\alpha_1 & 0 & -S\alpha_1 \\ 0 & 1 & 0 \\ S\alpha_1 & 0 & C\alpha_1 \end{pmatrix} \tag{10}$$

$$(\pi^1) = \begin{pmatrix} 1 & 0 & 0 \\ 0 & C\pi_1 & S\pi_1 \\ 0 & -S\pi_1 & C\pi_1 \end{pmatrix} \tag{11}$$

and explicitly

$$(A^1) = \begin{bmatrix} C\alpha_1 & 0 & -S\alpha_1 \\ S\pi_1 S\alpha_1 & C\pi_1 & S\pi_1 C\alpha_1 \\ C\pi_1 S\alpha_1 & -S\pi_1 & C\pi_1 C\alpha_1 \end{bmatrix} \tag{12}$$

+) S≡sin ; C≡cos

The components of the angular velocity $\vec{\Omega}^1$ are

$$(13) \qquad \begin{pmatrix} \Omega_x^1 \\ \Omega_y^1 \\ \Omega_z^1 \end{pmatrix} = \begin{pmatrix} \dot{\pi}_1 \\ \dot{\alpha}_1 \cos \pi_1 \\ -\dot{\alpha}_1 \sin \pi_1 \end{pmatrix}$$

4.12 Derivation of the Transformation (A^3)

Analogously to (8) there is the transformation

$$(14) \qquad \begin{pmatrix} X^3 \\ Y^3 \\ Z^3 \end{pmatrix} = (A^3) \begin{pmatrix} X^b \\ Y^b \\ Z^b \end{pmatrix}$$

between the orientation of the $X^bY^bZ^b$ and the $X^3Y^3Z^3$ coordinate systems. (A^3) is derived from two successive right hand rotations: through the angle β_3, about the Y^b axis, and through the angle π_3, about the Z^3 axis,

It is

$$(15) \qquad (A^3) = (\pi^3)(\beta^3)$$

where

$$(16) \qquad (\beta^3) = \begin{pmatrix} C\beta_3 & 0 & -S\beta_3 \\ 0 & 1 & 0 \\ S\beta_3 & 0 & C\beta_3 \end{pmatrix}$$

$$(17) \qquad (\pi^3) = \begin{pmatrix} C\pi_3 & S\pi_3 & 0 \\ -S\pi_3 & C\pi_3 & 0 \\ 0 & 0 & 1 \end{pmatrix}$$

and explicitly

$$(A^3) = \begin{pmatrix} C\pi_3 C\beta_3 & S\pi_3 & -C\pi_3 S\beta_3 \\ -S\pi_3 C\beta_3 & C\pi_3 & S\pi_3 S\beta_3 \\ S\beta_3 & 0 & C\beta_3 \end{pmatrix} \tag{18}$$

The componets of the angular velocity $\vec{\Omega}^3$ are

$$\begin{pmatrix} \Omega_x^3 \\ \Omega_y^3 \\ \Omega_z^3 \end{pmatrix} = \begin{pmatrix} \dot{\beta}_3 \sin \pi_3 \\ \dot{\beta}_3 \cos \pi_3 \\ \dot{\pi}_3 \end{pmatrix} \tag{19}$$

4.13 Expressions for the Angular Momentum Vectors

4.131 Carrier

In order to establish the equations of motion of the carrier, the components of the carrier angular momentum vector $\vec{L}$ have first to be expressed in the XYZ coordinate system. With this in mind one obtains from (3), if the third term in that formula is omitted, in matrix notation the expression

$$\begin{aligned} (L) = \{(I^b) + (A^1)^{-1}(I^1)(A^1) + (A^3)^{-1}(I^3)(A^3)\}(\Omega) \\ + (A^1)^{-1}(I^1)(\Omega^1) + (A^3)^{-1}(I^3)(\Omega^3) \end{aligned} \tag{20}$$

where $(A^1)^{-1}$ and $(A^3)^{-1}$ are the inverse matrices of (A^1) and (A^3), respectively. It is assumed that

$$(I^b) = \begin{pmatrix} I_{xx}^b & 0 & 0 \\ 0 & I_{yy}^b & 0 \\ 0 & 0 & I_{zz}^b \end{pmatrix} \tag{22}$$

$$(22) \qquad (I^1) = \begin{pmatrix} I^1_{xx} & 0 & 0 \\ 0 & I^1_{yy} & 0 \\ 0 & 0 & I^1_{zz} \end{pmatrix} = \begin{pmatrix} I_S & 0 & 0 \\ 0 & I_T & 0 \\ 0 & 0 & I_T \end{pmatrix}$$

and accordingly for the case of identical CMGs

$$(23) \qquad (I^3) = \begin{pmatrix} I_T & 0 & 0 \\ 0 & I_T & 0 \\ 0 & 0 & I_S \end{pmatrix}$$

and

$$I^b_{xx} >> I_S(\cos^2\alpha_1 + \sin^2\beta_2) + I_T(\sin^2\alpha_1 + \cos^2\beta_3),$$

$$I^b_{zz} >> I_S(\sin^2\alpha_1 + \cos^2\beta_3) + I_T(\cos^2\alpha_1 + \sin^2\beta_3)$$

and

$$I^b_{yy} >> 2I_T$$

$$H_1 = H_3 \equiv H$$

where

$$H_1 = I_S\dot{\pi}_1 \quad , \quad H_3 = I_S\dot{\pi}_3$$

Then from (20) the components of $\vec{L}$ are explicitly

$$(24) \qquad \begin{pmatrix} L_x \\ I_y \\ L_z \end{pmatrix} = \begin{bmatrix} I^b_{xx} & 0 & C_1(S2\beta_3 - S2\alpha_1) \\ 0 & I^b_{yy} & 0 \\ C_1(S2\beta_3 - S2\alpha_1) & 0 & I^b_{zz} \end{bmatrix} \begin{bmatrix} \Omega_x \\ \Omega_y \\ \Omega_z \end{bmatrix}$$

$$+ H \begin{pmatrix} C\alpha_1 + S\beta_3 \\ 0 \\ C\beta_3 - S\alpha_1 \end{pmatrix} + I_T \begin{pmatrix} 0 \\ \dot{\alpha}_1 + \dot{\beta}_3 \\ 0 \end{pmatrix}$$

where

$$C_1 = \tfrac{1}{2}(I_S - I_T)$$

4.132 Control Moment Gyros

In matrix notation and referred to the respective CMG coordinates the following expressions for the components of $\vec{L}^1$ and $\vec{L}^3$ are obtained from (6), observing (8) and (14)

$$(25) \qquad (L^1) = (I^1)\,[(\Omega^1) + (A^1)(\Omega)]$$

$$(26) \qquad (L^3) = (I^3)\,[(\Omega^3) + (A^3)(\Omega)]$$

4.14 Equations of Motion

The exact equations for the attitude motion of the carrier and the equations of motion for the CMGs are derived

from (24), (25), (26) according to (5) and (6), respectively. For the carrier one obtains explicitly

$$N_x = I^b_{xx}\dot{\Omega}_x + C_1\{[\dot{\Omega}_z + \Omega_x\Omega_y][S2\beta_3 - S2\alpha_1]$$
$$+ 2\Omega_z[\dot{\beta}_3 C2\beta_3 - \dot{\alpha}_1 C2\alpha_1]\} + \Omega_y\Omega_z[I^b_{zz} - I^b_{yy}] \tag{27}$$
$$- \Omega_z I_T[\dot{\alpha}_1 + \dot{\beta}_3] + H\{[\Omega_y + \dot{\beta}_3]C\beta_3 - [\Omega_y + \dot{\alpha}_1]S\alpha_1\}$$

$$N_y = I^b_{yy}\dot{\Omega}_y + I_T[\ddot{\alpha} + \ddot{\beta}_3] + C_1[\Omega_z^2 - \Omega_x^2][S2\beta_3 - S2\alpha_1]$$
$$+ \Omega_x\Omega_z[I^b_{xx} - I^b_{zz}] + H\{\Omega_x[S\alpha_1 - C\beta_3] + \Omega_z[C\alpha_1 + S\beta_3]\} \tag{28}$$

$$N_z = I^b_{zz}\dot{\Omega}_z + C_1\{[\dot{\Omega}_x - \Omega_y\Omega_z][S2\beta_3 - S2\alpha_1] + 2\Omega_x(\dot{\beta}_3 C2\beta_3$$
$$- \dot{\alpha}_1 C2\alpha_1]\} + \Omega_x\Omega_y[I^b_{yy} - I^b_{xx}] + \Omega_x I_T[\dot{\alpha}_1 + \dot{\beta}_3]$$
$$- H\{[\Omega_y + \dot{\alpha}_1]C\alpha_1 + [\Omega_y + \dot{\beta}_3]S\beta_3\} \tag{29}$$

The equations of motion for the two CMGs about the respective gimbal axes are

$$0 = I_T[\ddot{\alpha}_1 + \dot{\Omega}_y] + H[\Omega_z C\alpha_1 + \Omega_x S\alpha_1]$$
$$+ [I_S - I_T]\{[\Omega_x^2 - \Omega_z^2]\tfrac{1}{2} S2\alpha_1 + \Omega_x\Omega_z C2\alpha_1\} \tag{30}$$
$$+ \text{friction terms}$$

$$0 = I_T[\ddot{\beta}_3 + \dot{\Omega}_y] + H[\Omega_z S\beta_3 - \Omega_x C\beta_3]$$
$$+ [I_S - I_T]\{[\Omega_z^2 - \Omega_x^2]\tfrac{1}{2} S2\beta_3 - \Omega_x\Omega_z C2\beta_3\} \tag{31}$$
$$+ \text{friction terms}$$

Retaining only the major terms in (27) through (31) yields the following set of 5 equations which together describe finally the attitude motion of the carrier.

$$N_x = I^b_{xx}\dot{\Omega}_x + \Omega_y\Omega_z[I^b_{zz} - I^b_{yy}] + H\{[\Omega_y + \dot{\beta}_3]C\beta_3 - [\Omega_y + \dot{\alpha}_1]S\alpha_1\} \tag{32}$$

$$N_y = I^b_{yy}\dot{\Omega}_y + \Omega_x\Omega_z[I^b_{xx} - I^b_{zz}] + H\{\Omega_z[C\alpha_1 + S\beta_3] + \Omega_x[S\alpha_1 - C\beta_3]\} \tag{33}$$

$$N_z = I^b_{zz}\dot{\Omega}_z + \Omega_x\Omega_y[I^b_{yy} - I^b_{xx}] - H\{[\Omega_y + \dot{\beta}_3]S\beta_3 + [\Omega_y + \dot{\alpha}_1]C\alpha_1\} \tag{34}$$

$$0 = I_T\ddot{\alpha}_1 + H[\Omega_x S\alpha_1 + \Omega_z C\alpha_1] + \text{friction terms} \tag{35}$$

$$0 = I_T\ddot{\beta}_3 + H[\Omega_z S\beta_3 - \Omega_x C\beta_3] + \text{friction terms} \tag{36}$$

4.2 The 1-CMG Configuration

The following equations of motion for this case hold for a configuration as it is shown in Figure 3 or Figure 4 except that $\vec{H}_3$ is zero now. Again, only the terms of major influence have been retained [4]

$$N_x = I^b_{xx}\dot{\Omega}_x + \Omega_y\Omega_z[I^b_{zz} - I^b_{yy}] - H[\Omega_y + \dot{\alpha}_1]S\alpha_1 \tag{37}$$

$$N_y = I^b_{yy}\dot{\Omega}_y + \Omega_x\Omega_z[I^b_{xx} - I^b_{zz}] + H[\Omega_x S\alpha_1 + \Omega_z C\alpha_1] \tag{38}$$

$$N_z = I^b_{zz}\dot{\Omega}_z + \Omega_x\Omega_y[I^b_{yy} - I^b_{xx}] - H[\Omega_y + \dot{\alpha}_1]C\alpha_1 \tag{39}$$

$$0 = I_T\ddot{\alpha}_1 + H[\Omega_x S\alpha_1 + \Omega_z C\alpha_1] + \text{friction terms} \tag{40}$$

4.3 The 3-CMG Configuration

Analogously the equations of motion for a 3-CMG configuration can be obtained. Here they are presented for the case shown in Figure 5. The spin angular momentum vector $\vec{H}_2$ of the third CMG can move in the Y^bZ^b coordinate plane. The gimbal angular velocity $\dot{\beta}_2$ is parallel to the X^b axis. The equations are [4], again retaining the major terms,

$$N_x = I^b_{xx}\dot{\Omega}_x + \Omega_y\Omega_z[I^b_{zz} - I^b_{yy}] + H\{[\Omega_y + \dot{\beta}_3]C\beta_3 - [\Omega_y + \dot{\alpha}_1]S\alpha_1 + \Omega_y S\beta_2 - \Omega_z C\beta_2\} \tag{41}$$

$$N_y = I^b_{yy}\dot{\Omega}_y + \Omega_x\Omega_z[I^b_{xx} - I^b_{zz}] + H\{\Omega_x S\alpha_1 - [\Omega_x + \dot{\beta}_2]S\beta_2 - \Omega_x C\beta_3 + \Omega_z[C\alpha_1 + S\beta_3]\} \tag{42}$$

$$N_z = I^b_{zz}\dot{\Omega}_z + \Omega_x\Omega_y[I^b_{yy} - I^b_{xx}] + H\{[\Omega_x + \dot{\beta}_2]C\beta_2 - [\Omega_y + \dot{\alpha}_1]C\alpha_1 - [\Omega_y + \dot{\beta}_3]S\beta_3\} \tag{43}$$

$$0 = I_T\ddot{\alpha}_1 + H[\Omega_x S\alpha_1 + \Omega_z C\alpha_1] + \text{friction terms} \tag{44}$$

$$0 = I_T\ddot{\beta}_2 + H[\Omega_y S\beta_2 - \Omega_z C\beta_2] + \text{friction terms} \tag{45}$$

$$0 = I_T\ddot{\beta}_3 + H[\Omega_z S\beta_3 - \Omega_x C\beta_3] + \text{friction terms} \tag{46}$$

5.0 DERIVATION OF LINEAR MODELS

5.1 Linearization and Laplace Transformation of the Exact Equations of Motion

From the equations of motion which have been established for various CMG configurations, linear expression are now obtained. Subsequently they are Laplace-transformed. These expressions are the basis for the linear models.

First the equations of motion are linearized by Taylor series expansions about certain initial values of the respective variables which are marked by the index 0, namely in this paper

$$(47) \qquad \begin{pmatrix} \alpha_{10} \\ \beta_{20} \\ \beta_{30} \end{pmatrix} = \begin{pmatrix} 0 \\ 0 \\ -\pi/2 \end{pmatrix} \quad ; \quad \begin{pmatrix} \Omega_{x0} \\ \Omega_{y0} \\ \Omega_{z0} \end{pmatrix} = 0 \quad ; \quad \begin{pmatrix} \dot{\alpha}_{10} \\ \dot{\beta}_{20} \\ \dot{\beta}_{30} \end{pmatrix} = 0$$

As for the friction terms, it is assumed that they can be represented by speed proportional viscous friction terms. Thus, $D_1\dot{\alpha}_1$, $D_2\dot{\beta}_2$ and $D_3\dot{\beta}_3$ are these terms for the α_1, β_2 and β_3 gimbal axis, respectively. However, in Chapter 6, it will be shown how Coulomb friction phenomena can also be incorporated in these models. The results of executing the previously described steps can be represented by the following expression where the index j, (j = I,II,III), refers to the 1- , 2- and 3-CMG configuration, respectively.+)

$$(48) \qquad (n^j(s)) = (T^j(s))(\omega^j(s))$$

where

$$(n^I(s)) = \begin{pmatrix} n_x(s) \\ n_y(s) \\ n_z(s) \\ 0 \end{pmatrix} \quad ; \quad (n^{II}(s)) = \begin{pmatrix} n_x(s) \\ n_y(s) \\ n_z(s) \\ 0 \\ 0 \end{pmatrix} \quad ; \quad (n^{III}(s)) = \begin{pmatrix} n_x(s) \\ n_y(s) \\ n_z(s) \\ 0 \\ 0 \\ 0 \end{pmatrix}$$

+) s is the operator of the Laplace transform. All variables in the time domain, except for the gimbal variables $\alpha_1^{(n)}$, $\beta_2^{(n)}$, $\beta_3^{(n)}$ are represented by capital letters; transformed variables by small letters [5].

$$(\omega^{I}(s)) = \begin{pmatrix} \omega_x(s) \\ \omega_y(s) \\ \omega_z(s) \\ \dot{\alpha}_1(s) \end{pmatrix}; \quad (\omega^{II}(s)) = \begin{pmatrix} \omega_x(s) \\ \omega_y(s) \\ \omega_z(s) \\ \dot{\alpha}_1(s) \\ \dot{\beta}_3(s) \end{pmatrix}; \quad (\omega^{III}(s)) = \begin{pmatrix} \omega_x(s) \\ \omega_y(s) \\ \omega_z(s) \\ \dot{\alpha}_1(s) \\ \dot{\beta}_2(s) \\ \dot{\beta}_3(s) \end{pmatrix}$$

$$(T^{I}(s)) = \begin{bmatrix} I^b_{xx}s & 0 & 0 & 0 \\ 0 & I^b_{yy}s & H & 0 \\ 0 & -H & I^b_{zz}s & -H \\ 0 & 0 & H & I_T s + D_1 \end{bmatrix}$$

$$(T^{II}(s)) = \begin{bmatrix} I^b_{xx}s & 0 & 0 & 0 & 0 \\ 0 & I^b_{yy}s & 0 & 0 & 0 \\ 0 & 0 & I^b_{zz}s & -H & H \\ 0 & 0 & H & I_T s + D_1 & 0 \\ 0 & 0 & -H & 0 & I_T s + D_3 \end{bmatrix}$$

$$(T^{III}(s)) = \begin{bmatrix} I^b_{xx}s & 0 & -H & 0 & 0 & 0 \\ 0 & I^b_{yy}s & 0 & 0 & 0 & 0 \\ H & 0 & I^b_{zz}s & -H & H & H \\ 0 & 0 & H & I_T s + D_1 & 0 & 0 \\ 0 & 0 & -H & 0 & I_T s + D_2 & 0 \\ 0 & 0 & -H & 0 & 0 & I_T s + D_3 \end{bmatrix}$$

5.2 Transfer Functions and Eigenfrequencies

From (48), the general expression for the transfer functions which relate the variables of the matrices $(\omega^j(s))$ to the external torque matrices $(n^j(s))$, one obtains

$$(49) \qquad (\omega^j(s)) = (T^j(s))^{-1}(n^j(s))$$

where $(T^j(s))^{-1}$ is the inverse form of $(T^j(s))$. It will be shown later how Coulomb friction affects the behavior of such a system. Here it suffices to say that depending on the values of the Coulomb friction terms ,the carrier must first have attained an angular velocity in order that motion or a breakaway of the gimbals is possible. With this in mind and assuming a simultaneous breakway of all gimbals, one obtains for a certain CMG configuration 2 sets of transfer functions. The first set describes the behavior of the respective system as long as no breakway has occured. Then the variables $\alpha_1(t)$, $\beta_2(t)$ and $\beta_3(t)$ are constants and no motion about the gimbals occurs. The $(T^j(s))$ matrices are reduced to 3 x 3 matrices. Here they are marked by a star index, i.e., $(T_*^j(s))$.

The second set of transfer functions holds for the system after breakaway has occured.

If breakaway does not occur simultaneously for all gimbals, more sets of transfer functions are necessary to describe the system's behavior. One can provide for this analytically by suitable linearizations of the exact equations of motion.

Furthermore, the breakway-go-stop-etc. behavior of a gimbal which is a characteristic phenomenon of Coulomb friction can, as it will be seen, also be represented by suitably chosen transfer functions.

Assuming that the viscous friction terms are zero, the following Eigenfrequencies Ω_e^j are obtained from (48)

a) from matrices $(T_*^j(s))$, before breakaway

$$(50) \qquad \Omega^I{}_e = \frac{H}{[I^b_{yy} I^b_{zz}]^{1/2}} \quad ; \quad \Omega_e^{II} = 0 \quad ; \quad \Omega_e^{III} = \frac{H}{[I^b_{xx} I^b_{zz}]^{1/2}}$$

(b) from matrices $(T^j(s))$, after breakaway

$$(51) \qquad \Omega_e^I = \frac{H}{[I_{zz}^b I_T]^{1/2}} \quad ; \quad \Omega_e^{II} = H\left(\frac{2}{I_{zz}^b I_T}\right)^{1/2}$$

$$\Omega_e^{III} = H\left(\frac{3}{I_{zz}^b I_T)}\right)^{1/2}$$

Thus there is the ratio for the frequencies of (51)

$$(52) \qquad \Omega_e^I : \Omega_e^{II} : \Omega_e^{III} = 1 : \sqrt{2} : \sqrt{3}$$

Comparing the values of Ω_e^j in (50) with those of (51), one notes the significant difference between the Eigenfrequencies. Those of (51) are, in general, much higher.

If viscous friction is present, the resulting expressions are too complicated to show explicity in general form.

Figure 6 is a representation of the transfer functions for the 1-CMG configuration. As long as no breakaway of the gimbal has occured, this system is represented by the first three blocks where $\alpha_1 = 0$.

5.3 Influence of Viscous Friction Terms on Characteristic Equations

It is straightforward to obtain from (48) the Eigenfrequencies of the characteristic equations for CMG configurations with no viscous friction. However, for the general case having viscous friction, the relevant expressions are much more complicated. One of the most important items which can be derived from the characteristic equation is whether or not the system is stable. Therefore, in this section, the analysis is concerned with the influence of the viscous friction coefficients D_1, D_2 and D_3 on the stability of the respective systems with those CMG configurations. From the application of the Hurwitz stability criterion [6] to the characteristic equations obtained from (48), one can summarize the results as follows:

a) The 1-and 2-CMG configurations will always be stable for any values of the viscous friction coefficients D_1 and D_3.

b) With respect to the range of the investigations which have been carried out, the 3-CMG configuration will always be stable for any values in (ft. lb. sec) $D_1 \leq 1$, $D_2 \leq 1$, $D_3 \leq 1$. This configuration is probably stable for all values of the D's, but this has not been established analytically.

5.4 Accuracy of Linear Models

Of course, it is absolutely essential, to establish the accuracy the linear models (48) relative to the results obtained from the computer simulation of the exact equations of motion. It was found that for step and sinusoidal input functions, provided the gimbal angles did not exceed 10 degrees, those errors were less than 1%.

6.0 INFLUENCE OF COULOMB FRICTION

6.1 Friction as Function of Gimbal Angular Velocity

The models for the representation of the Coulomb friction coefficient F_σ as a function of the respective gimbal angular velocity are shown in Figure 7 and Figure 8. In Figure 7 the Coulomb friction coefficient F_σ has the constant value A_σ as function of the gimbal angular velocity $\dot{\sigma}$ and changes sign simultaneously with $\dot{\sigma}$. The behavior of F_σ in Figure 8 is somewhat different. However, this is a more precise model for the dependency of Coulomb friction on speed. The initial value or static friction level is again designated A_σ. After the gimbal angular velocity has attained the value $\dot{\sigma}_d$, the friction coefficient drops to the value B_σ and stays there for any $\dot{\sigma} > \dot{\sigma}_d$. For negative angular gimbal velocities the behavior is analogous. The combination of Coulomb and viscous friction yields the total frictional torque for a particular gimbal. The friction model according to Figure 8 together with a speed proportional viscous friction probably gives the simplest friction model which can be established without losing much accuracy. This statement is based on data which shows the actual behavior of friction for various types of bearings as a function of speed and bearing load, see in particular [7] page 178 and page 197.

Certainly, there is no sudden drop but, instead, a smooth transition from friction level A_σ to B_σ. Yet according to [7], this change occurs within a very small interval $\Delta\dot{\sigma}$ of the angular velocity. The advantage of introducing Coulomb friction in this way is twofold, namely, first it can be programmed easily for the computer simulations and secondly, this representation is probably the only one which is suitable for the linear analysis of the system.

As first impression from either Fig.7 or Fig. 8, one recognizes that for any value of $W(\alpha_1) < A_{\alpha_1}$, $W(\beta_2) < A_{\beta_2}$ and $W(\beta_3) < A_{\beta_3}$ in (35), (36); (40); or (44), (45) and (46) where

$$W(\alpha_1) \equiv H[\Omega_z \cos \alpha_1 + \Omega_x \sin \alpha_1]$$

$$W(\beta_2) \equiv H[\Omega_y \sin \beta_2 - \Omega_z \cos \beta_2] \tag{53}$$

$$W(\beta_3) \equiv H[\Omega_z \sin \beta_3 - \Omega_x \cos \beta_3]$$

there will be no motion about that particular gimbal. In order that a motion can start or the CMG can breakaway, the values $W(\sigma)$, $(\sigma = \alpha_1, \beta_2, \beta_3)$, must exceed A_σ. At this instant, the carrier has attained an angular velocity $\vec{\Omega}_b$. The breakaway condition can be formulated as

$$W(\sigma) \geq A_\sigma \tag{54}$$

Up to the time of gimbal breakaway the orientation of the relevant spin angular momentum vector is fixed with respect to the carrier, thus acting essentially as a fixed reaction body. This severely stricts the capability to stabilize the carrier's attitude.

Detailed information on this subject can be readily obtained, e.g., from the discussion in the previous Chapter 5. For the 2-CMG configuration the Coulomb friction phenomena prevents a stabilization effect before gimbal breakaway since the two CMGs stay at their initial orientation where the sum of spin angular momentums is zero. In this connection refer to Equations (50) and (51), which are expression for the Eigenfrequencies of the carrier.

It is of considerable interest to know that, depending on the value of A_σ and on the behavior of the external torque $\vec{N}$ as function of time, there may be no breakaway at all for a given CMG configuration. This can be illustrated by the following example. Assume a carrier and a 2-CMG configuration. The external torque may be given as

$$\vec{N} \equiv N_z = K \sin \Omega_o t$$

For instance, both, gravity-gradient torque and also the aerodynamic torque acting on a space vehicle which is in an orbit about the earth, can be represented by sinusoidal functions. Now the angular velocities about the vehicle's coordinate axes are obtained from (49). Explicitly it is $\omega_x(s)=0$, $\omega_y(s)=0$, but

$$\omega_z(s) = \frac{K\Omega_o}{I^b_{zz} s(s^2 + \Omega_o^2)} \tag{55}$$

or in the time domain

$$\Omega_z = \frac{K}{I^b_{zz}\Omega_o}(1 - \cos \Omega_o t) \tag{56}$$

Now from (56), (54) and (53), respectively, follows that if

$$A_\sigma > \frac{2HK}{I^b_{zz}\Omega_o} \tag{57}$$

the CMGs will not breakaway.

6.2 Examples of Coulomb Friction Influence on Attitude Motion

In order to illustrate the influence of Coulomb friction on the attitude of the carrier some simulation results obtained from equations (32) through (36) are presented. They hold for a carrier with a 2-CMG configuration. The external torque function $\vec{N}$ and the Coulomb friction coefficients F_σ are the variable parameters. At first, the constant parameters are listed:

$$(I^b) = 10^6 \begin{pmatrix} .3 & 0 & 0 \\ 0 & 2 & 0 \\ 0 & 0 & 2 \end{pmatrix} \text{ft. lb. sec}^2.; \; I_T = 1.2 \text{ ft. lb. sec}^2.$$

$$H = 2000 \text{ ft. lb. sec.}; \; A_\sigma = 0.06 \text{ ft. lb.}$$

Initially $\vec{H}_1$ and $\vec{H}_3$ are in the X^bY^b coordinate plane and the external torque has only a component about the vehicle's Z^b axis.

6.21 External Torque is Step Function

Figure 9 through Figure 13 show the carrier angular velocity Ω_z together with the gimbal angular velocity $\dot{\alpha}_1$ as functions of time with the variable parameter $F_\sigma, (\sigma = \alpha_1, \beta_3)$. The external torque is the step function

$$N_z = \begin{cases} 0 & ; \; t < 0 \\ 5 \text{ ft. lb.} & ; \; t \geq 0 \end{cases}$$

Furthermore, there is no viscous friction, i.e., $D_1 = 0_1$, $D_3 = 0$. Because of the nature of the input function and with the assumption $|F_{\alpha_1}| = |F_{\alpha_3}|$, it can be readily established that

$$\dot{\alpha}_1 = - \dot{\beta}_3 \quad , \quad \alpha_1 = -\beta_3$$

Therefore, it suffices to discuss the behavior of just one gimbal, there the α_1 gimbal. The calculation yields for the breakaway speed the value $\Omega_{zb} = 1.72 \times 10^{-3}$°/sec and breakaway occurs after 12 seconds. With respect to these figures the following explanation are offered:

Figure 9. F_σ = constant. After breakaway the angular velocities Ω_z and $\dot{\alpha}_1$ are

$$\Omega_z = \Omega_{zb} + 7.9\text{x}10^{-5} \sin \Omega_e^{II} t \,°/\text{sec}$$

$$\dot{\alpha}_1 = - 0.715\text{x}10^{-1} \cos (1-\Omega_e^{II} t) \,°/\text{sec}$$

where

$$\Omega_e^{II} = 1.83 \text{ 1/sec}$$

The second term of the first equation is shown separately on a larger scale. It would correspond to the time behavior of Ω_z if no Coulomb friction was present.

Figure 10. F_σ drops from the value A_σ = .06 ft. lb. to B_σ = 0.03 ft. lb. right at breakaway so that $\dot{\sigma}_d = 0$. At time t = 13.83 sec the gimbal stops as $\dot{\alpha}_1$ would change sign there. But no breakaway can occur now because $W(\alpha_1) < A_{\alpha_1}$. Therefore, the gimbal remains fixed in the particular angular position

$$\alpha_1 = \int_{t_b}^{t_s} \dot{\alpha}_1 dt$$

which it has attained now since breakaway. Subsequently the carrier is spun again by the external torque. Ω_z increases linearly until a new breakaway can occur, i.e., for $\Omega_z \geq \Omega_{zb}$. Comparing the maximum values of $\dot{\alpha}_1$ in both figures shows clearly the most significant influence of friction drop on the behavior of $\dot{\alpha}_1$. The ratio of the amplitudes amounts to $\dot{\alpha}_1$(Fig. 10)/ $\dot{\alpha}_1$ (Fig. 9) ≈ 6 here.

Figure 11 through Figure 13. Now the friction drop occurs at $\dot{\alpha}_1$ =-0.0034°/sec. The curves have been obtained for various values of B_σ namely (ft. lb), 0.05, 0.03 and 0.01 for Figures 11, 12, and 13, respectively. All Figures show the steep increase of the value of the gimbal angular velocity which begins the instant of the friction drop. Basically the behavior of the variables is the same. Especially from Figure 11 this typical pattern for the motion of the gimbals of the CMGs can be seen: breakaway, steep increase of gimbal angular velocity from time of friction drop, stop and subsequent gimbal rest, new breakaway etc.

6.22 External Torque is a Sine Function

The torque shall be given by the expression

$$N_z = 3.123 \sin(\Omega_o t - \Psi)$$

where $\Omega_o = 2.21352 \times 10^{-3}$ 1/sec. This frequency corresponds to twice the orbital rate of a space vehicle in a circular orbit at a height of 270 nautical miles and it takes 5677 seconds to complete one orbit. Figure 14 shows as the results of a computer simulation the external torque N_z together with Ω_z, Ψ, where $\dot{\Psi}=\Omega_z$, $W(\alpha_1)$, $\dot{\alpha}_1$, and α_1, respectively. It was assumed that D_1=0.1 ft. lb. and D_3=0.1 ft. lb. There is no drop in Coulomb friction. Again the motion of the β_3 gimbal is equal but opposite in sign with respect to the motion of the α_1 gimbal. The viscous friction now damps out the motion which is due to the Eigenfrequency of the system. The damping has the greatest influence on the time behavior of $\dot{\alpha}$. This can be seen from the spikes in $\dot{\alpha}_1(t)$ where in order to facilitate the drawing, only the highest and the lowest values of $\dot{\alpha}_1$ have been indicated.

This Eigenfrequency effect is also present with the variables Ω_Z and $W(\alpha_1)$, but in it is so minor that it does not show up in the figure. That is a consequence of the high value of the breakaway angular velocity Ω_{zb}.

All the phenomena which have been described can readily be derived from linear analysis, i.e., from Equation (49).

6.3 Attitude Error and Coulomb Friction Drop

Let $X^rY^rZ^r$ be an inertially fixed right hand Cartesian coordinate system and (D), (D)=(Φ)(Θ)(Ψ), a transformation matrix with the three Euler angles Ψ, Θ, Φ such that [4]

$$\begin{pmatrix} X \\ Y \\ Z \end{pmatrix} = (D) \begin{pmatrix} X^r \\ Y^r \\ Z^r \end{pmatrix}$$

and the components of the carrier's angular velocity $\vec{\Omega}$ are given in terms of these Euler angles as

$$\Omega_x = \dot{\phi} - \dot{\psi}\sin\theta$$

$$\Omega_y = \dot{\theta}\cos\phi + \dot{\psi}\sin\phi\cos\theta \tag{59}$$

$$\Omega_z = -\dot{\theta}\sin\phi + \dot{\psi}\cos\phi\cos\theta$$

so that for small angles (59) may be approximated

$$\Omega_x \approx \dot{\phi}$$

$$\Omega_y \approx \dot{\theta} \tag{60}$$

$$\Omega_z \approx \dot{\psi}$$

It follows from the discussions in the previous two Sections 6.21 and 6.22 where only Ω_z was present that the angular deflection or attitude error $\Delta\Psi$ of the carrier

$$\Delta\Psi = \Psi(t) - \Psi_0 = \int_0^t \Omega_z dt \tag{61}$$

had as function of F_σ its maximum value when no friction drop occurred. Thus the case of having a constant value for F_σ yielded an upper bound for $\Delta\Psi$.

Obviously this statement can now be generalized at least for all cases where the approximation (60) holds.

7.0 EXTENSION OF LINEAR MODEL TO INCLUDE COULOMB FRICTION

The linear models which have been derived in Chapter 5 can be extended to include the previously described Coulomb friction phenomena. Here the extension will be presented for the cases which are discussed in Section 6.2 and are shown in Figure 9 through Figure 14. Analogously, the respective linear models can be obtained also for other cases. But, in general, it can be noted that except for simple or special cases the linear models will probably turn out to be too complicated and too laborious for explicit evaluations without using computers.

Such a linear model is established in sections. The first section covers the interval from the beginning of the angular motion of the carrier at time zero until gimbal breakaway occurs at $t=t_b$. Subsequently follows the section from time of gimbal breakaway to the instant of Coulomb friction drop at $t=t_d$. The third section starts here and ends at time $t=t_s$, when the gimbals come to a stop. With the fourth section this cycle starts again with the spinning up of the carrier until gimbal breakaway occurs again.

Explicitly one obtains now:

Section 1: $0 \leq t < t_b$

$$(62) \qquad \begin{pmatrix} 0 \\ 0 \\ \omega_z(s) \end{pmatrix} = (T_*^{II}(s))^{-1} \begin{pmatrix} 0 \\ 0 \\ n_z(s) \end{pmatrix}$$

where for $t=t_b$

$$(\Omega) = \begin{pmatrix} 0 \\ 0 \\ \Omega_{zb} \end{pmatrix}$$

Section 2: $t_b \leq t < t_d$

$$(63) \qquad (\omega(s)) = \frac{\Omega_{zb}}{s} + e^{-st_b}(T^{II}(s))^{-1}(n(s))$$

where

$$(\omega(s)) = \begin{pmatrix} 0 \\ 0 \\ \omega_z(s) \\ \dot{\alpha}_1(s) \\ \dot{\beta}_3(s) \end{pmatrix}; \quad (n(s)) = \begin{pmatrix} 0 \\ 0 \\ n_z(s) \\ 0 \\ 0 \end{pmatrix}$$

and

a) for the case of having the step function torque, Figure 9 through Figure 13

$$n_z(s) = \frac{n_z}{s}$$

b) for the sine function input, Figure 14

$$N_z = 3.12 \sin(\Omega_o t + \Gamma_b - \Psi) \quad ; \quad \Gamma_b = \Omega_o t_b$$

Because at time $t=t_b$, $\Psi \approx 0.2°$. Therefore, it can be neglected.

Thus

$$N_z = 3.12 \sin(\Omega_o t + \Gamma_b)$$

and [5]

$$n_z(s) = 3.12 \left(\frac{\Omega_o \cos \Gamma_b + s \sin \Gamma_b}{s^2 + \Omega_o{}^2} \right)$$

Section 3: $t_d \leq t < t_s$

$$(\omega(s)) = \frac{\Omega_{zb}}{s} + e^{-st_b}(T^{II}(s))(n(s))$$

$$+ e^{-st_d}(T^{II}(s)) \begin{pmatrix} 0 \\ 0 \\ 0 \\ C_{\alpha_1} \\ C_{\beta_3} \end{pmatrix}$$

where

$$C_{\alpha_1} = A_{\alpha_1} - B_{\alpha_1}$$

$$C_{\beta_3} = A_{\beta_3} - B_{\beta_3}$$

i.e., because $\dot{\alpha}_1$, is negative, C_{α_1} will be negative here, and analogously, C_{β_3} will have a positive sign. It is further assumed that during time interval $t_b \leq t \leq t_d$ the changes of the respective variables are so small that the matrix $(T^{II}(s))$ from the previous section 2 can also be used.

Section 4: $t > t_s$

New spin up of the carrier with both gimbals at rest until next gimbal breakaway can occur.

Compared with the computer runs, the accuracy of the results which were obtained from this linear model is such that the errors are less than 1%.

8.0 ACKNOWLEDGMENT

The author sincerely wishes to thank B. D. Elrod, C. O. Guffee, and J. Kranton for their invaluable suggestions and assistance during the preparation of this paper.

1022-JWS-mef

J. W. Schindelin

Attachments
References
Figures 1-14

REFERENCES

[1] Bendix Eclipse Pioneer Division, Teterboro, N. J. MT-14, 101, 1967: The Description of the CMG and its Application to Space Vehicle Control.

[2] Schindelin, J. W.: Bewegungsgleichungen eines „Systems gekoppelter starrer Flugkörper. Zeitschrift für Flugwissenschaften, 15, (1967), No. 11, pp. 432-434.

[3] Goldstein, H.: Classical Mechanics. Addison-Wesley Publishing Co., Inc., 1956, 4th printing.

[4] Elrod, B. and J. Kranton: Unpublished notes on the Stabilization of space vehicles by CMGs. Bellcomm, Inc., 1967.

[5] Doetsch, G.: Anleitung zum praktischen Gebrauch der Laplace-Transformation. R. Oldenbourg, Munich, 1956.

[6] Solowdownikow, W. W.: Grundlagen der selbsttaetigen Regelung. Vol. I., R. Oldenbourg, Munich, 1959.

[7] Akademischer Verein Huette, E. V. (editor): Huette, Vol. II, 27th printing. Wilhelm Ernst and Sohn, Berlin, 1949.

[8] Schindelin, J. W.: AAP-Cluster Stabilization by Passive Control Moment Gyros. Bellcomm, Inc. TM-68-1022-7.

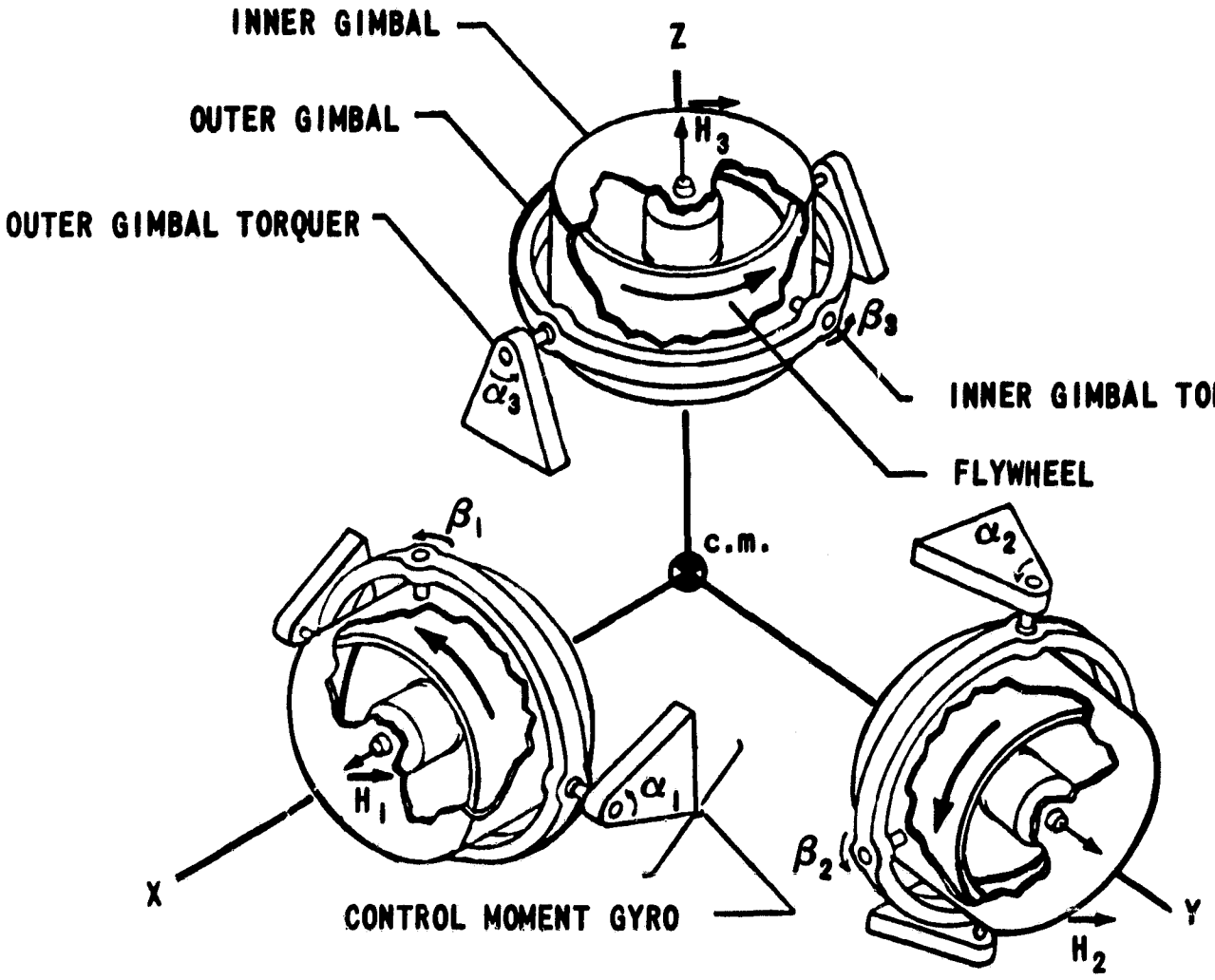

FIGURE I - SIXPAC CMG CONFIGURATION

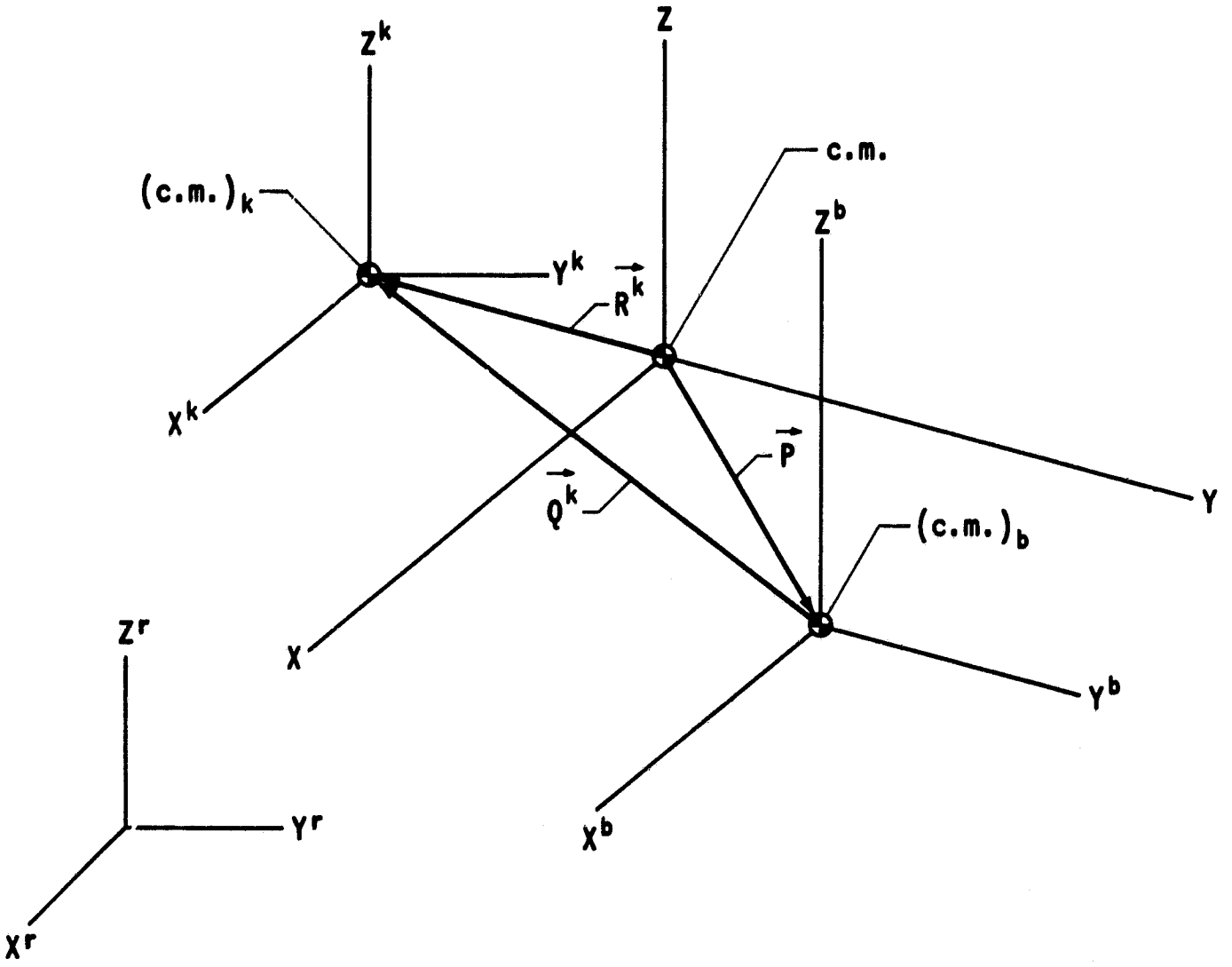

FIGURE 2 - COORDINATE SYSTEMS AND VECTORS

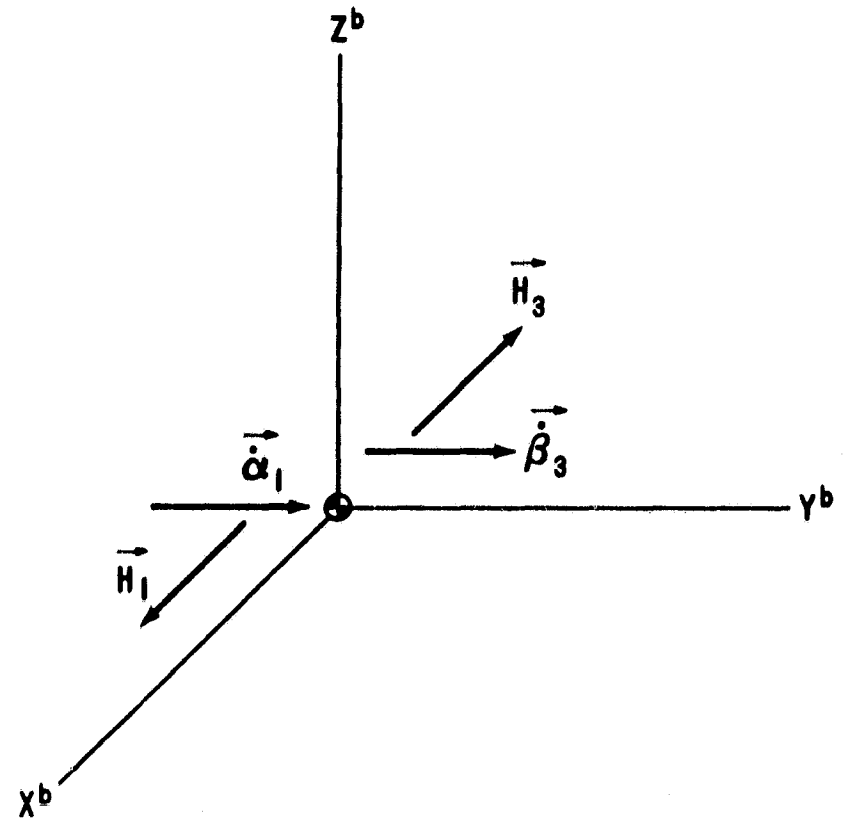

FIGURE 3 - 2-CMG CONFIGURATION. ORIENTATION OF SPIN ANGULAR MOMENTUM AND GIMBAL ANGULAR VELOCITY VECTORS

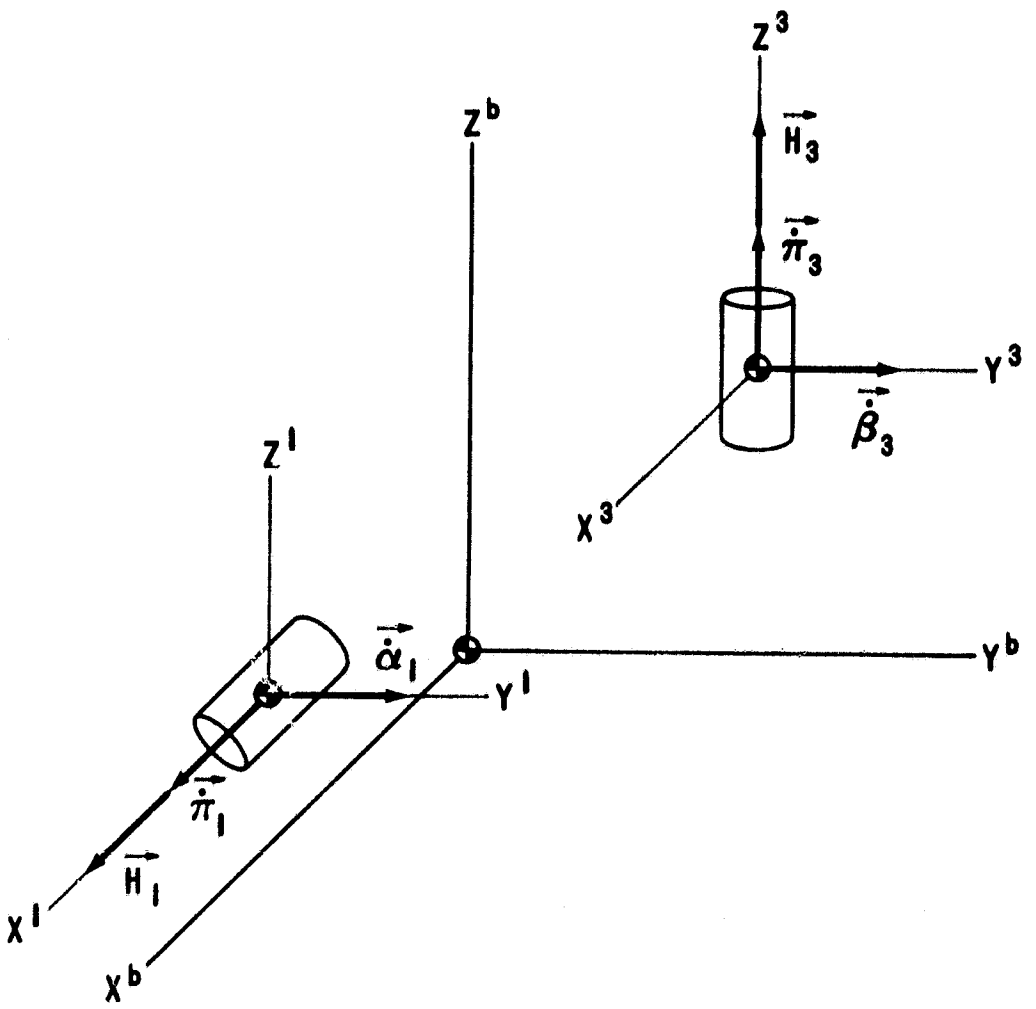

FIGURE 4 - DERIVATION OF THE TRANSFORMATIONS (A^1) AND (A^3)

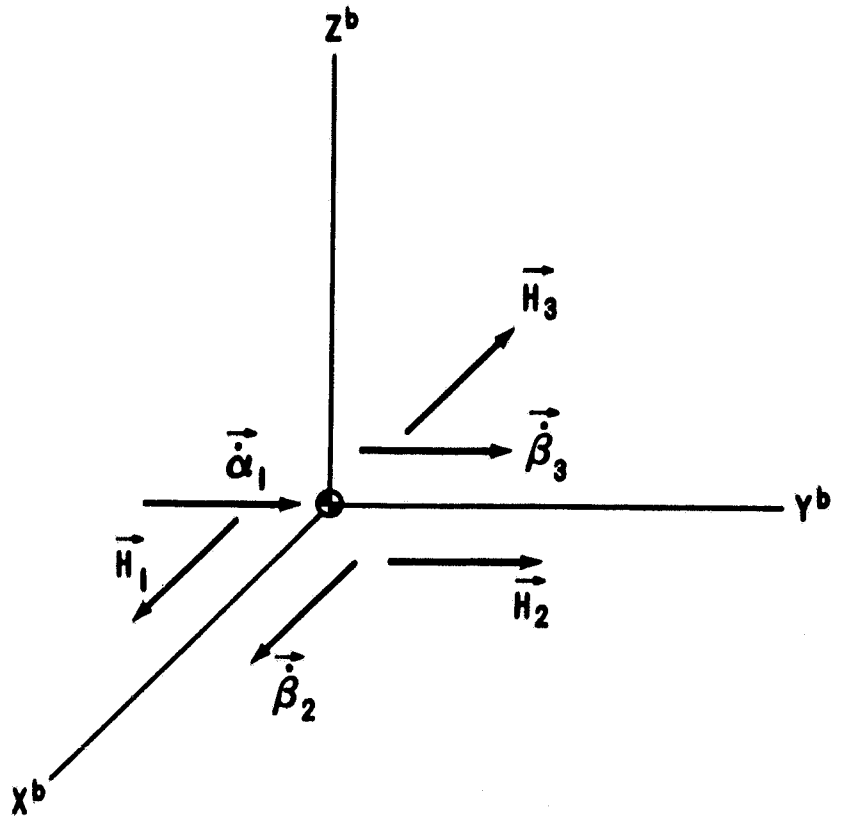

FIGURE 5 - 3-CMG CONFIGURATION. ORIENTATION OF SPIN ANGULAR MOMENTUM AND GIMBAL ANGULAR VELOCITY VECTORS

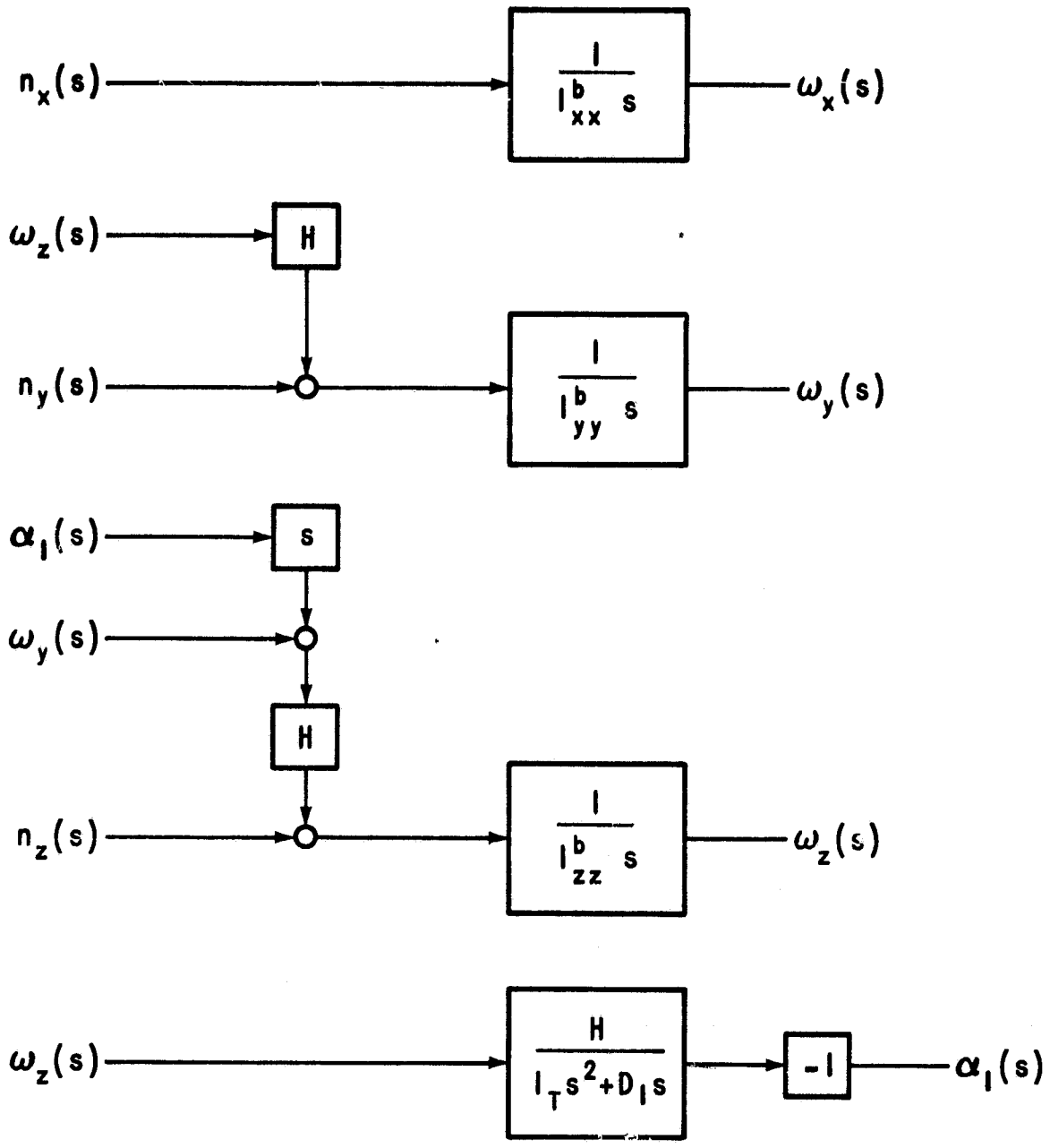

FIGURE 6 – TRANSFER FUNCTION FOR THE 1-CMG CONFIGURATION

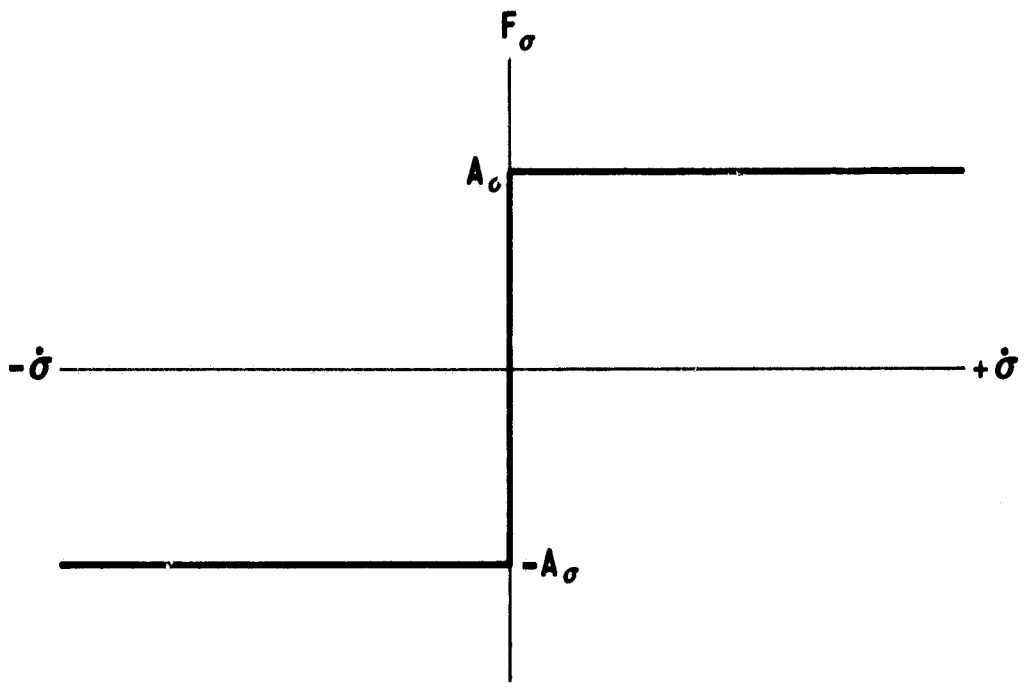

FIGURE 7 - COULOMB FRICTION COEFFICIENT F_σ VS GIMBAL ANGULAR VELOCITY $\dot{\sigma}$ WITH NO FRICTION DROP

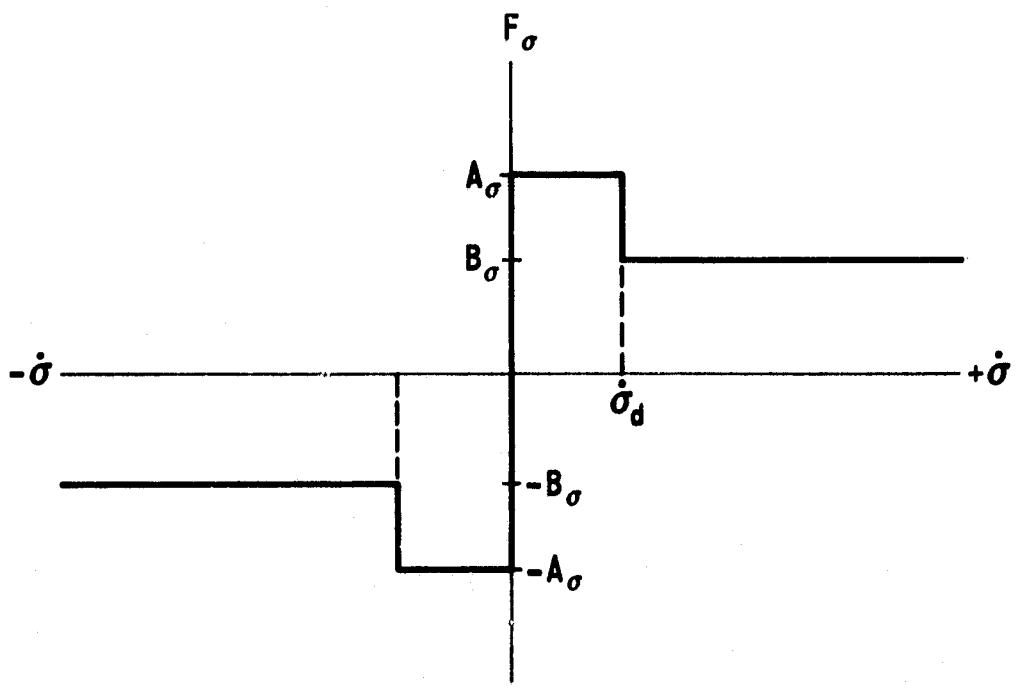

FIGURE 8 - COULOMB FRICTION COEFFICIENT F_σ VS GIMBAL ANGULAR VELOCITY $\dot{\sigma}$ WITH FRICTION DROP

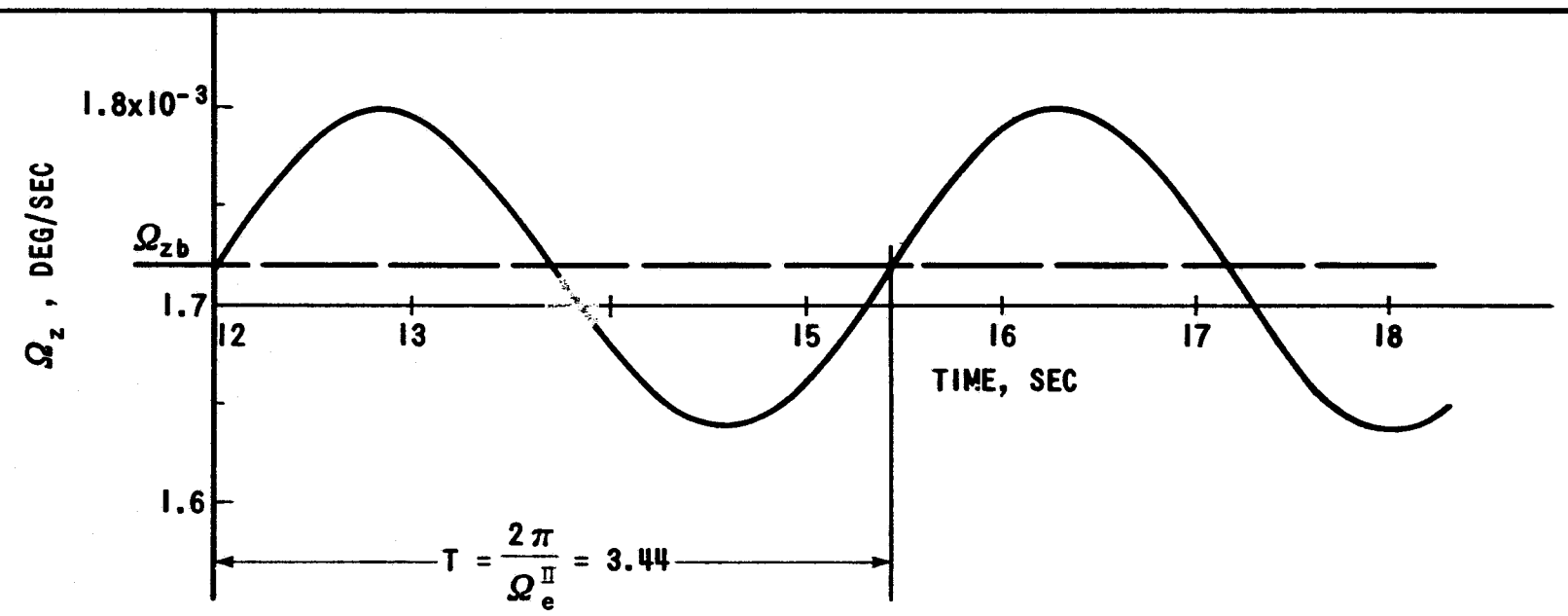

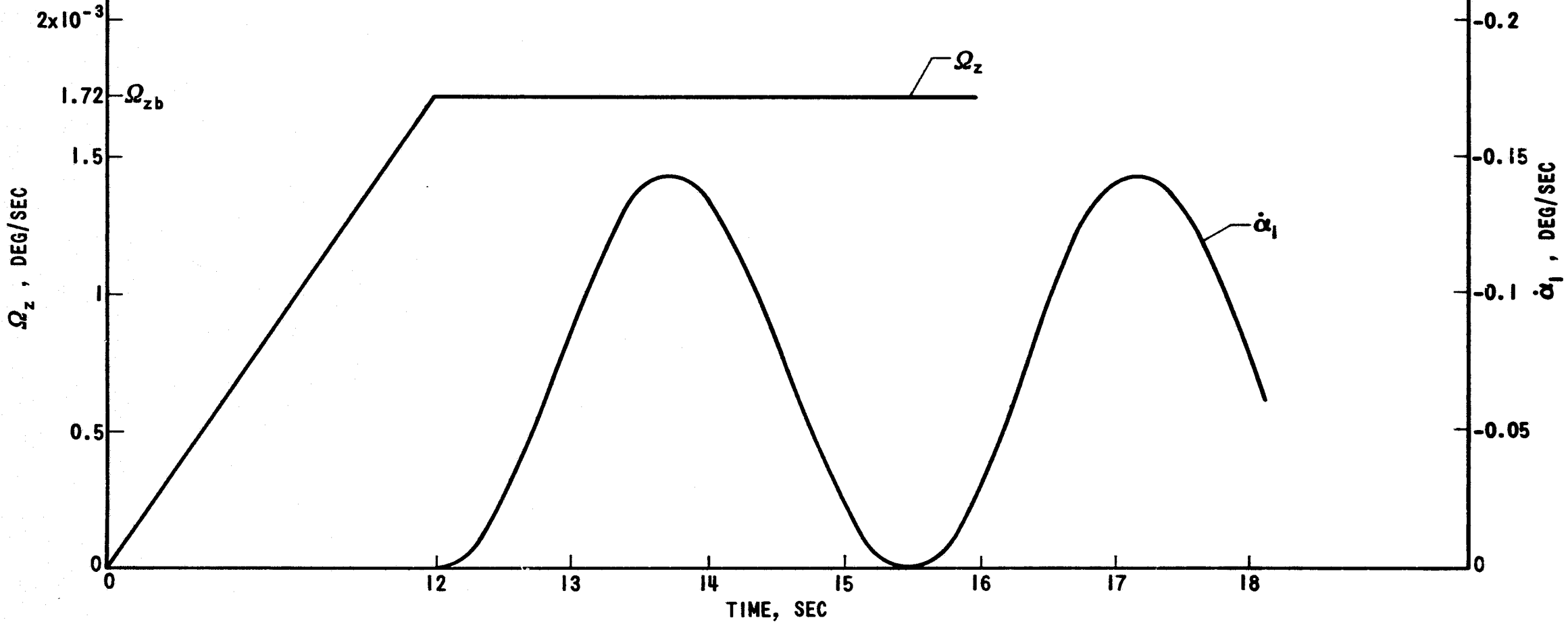

FIGURE 9 - NO COULOMB FRICTION DROP. ANGULAR VELOCITIES Ω_z AND $\dot{\alpha}_1$ AS FUNCTIONS OF TIME

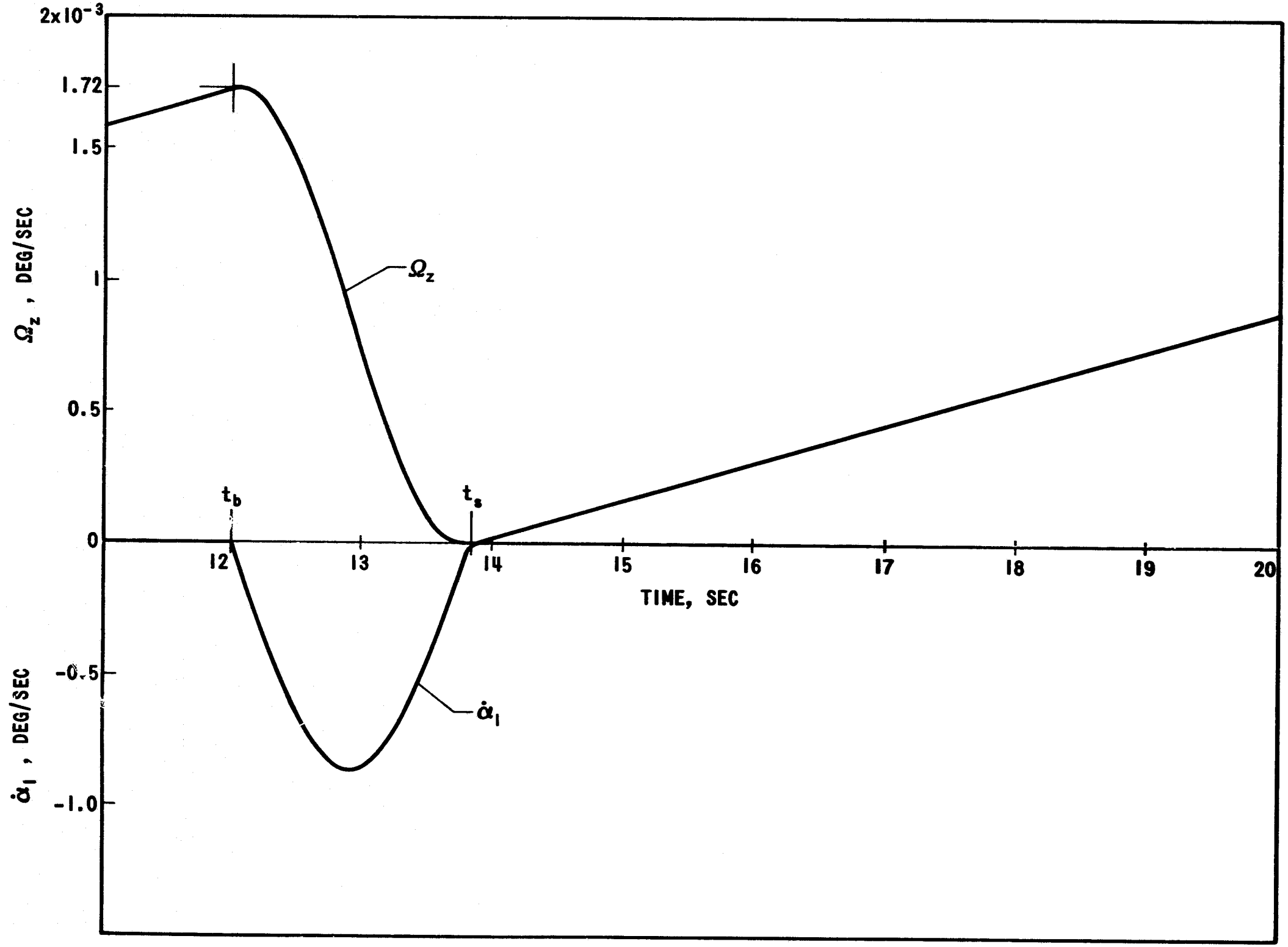

FIGURE 10 - COULOMB FRICTION DROP AT GIMBAL BREAKAWAY. ANGULAR VELOCITIES Ω_z AND $\dot{\alpha}_1$ AS FUNCTIONS OF TIME

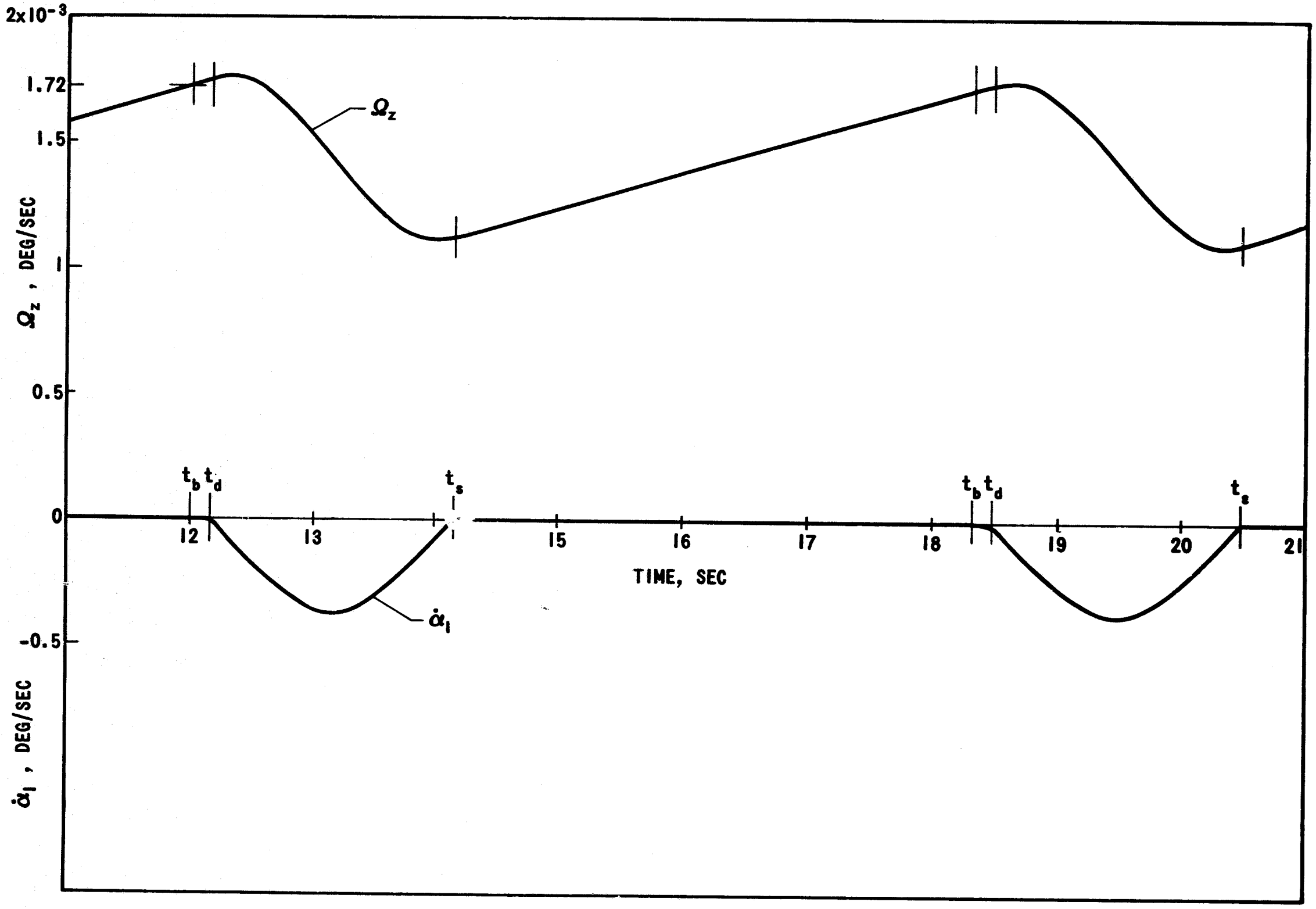

FIGURE 11 - COULOMB FRICTION DROP AT $\dot{\alpha}_l$ = -0.0034 DEG/SEC. B_σ = 0.05 FT.LB. ANGULAR VELOCITIES Ω_z AND $\dot{\alpha}_l$ AS FUNCTIONS OF TIME

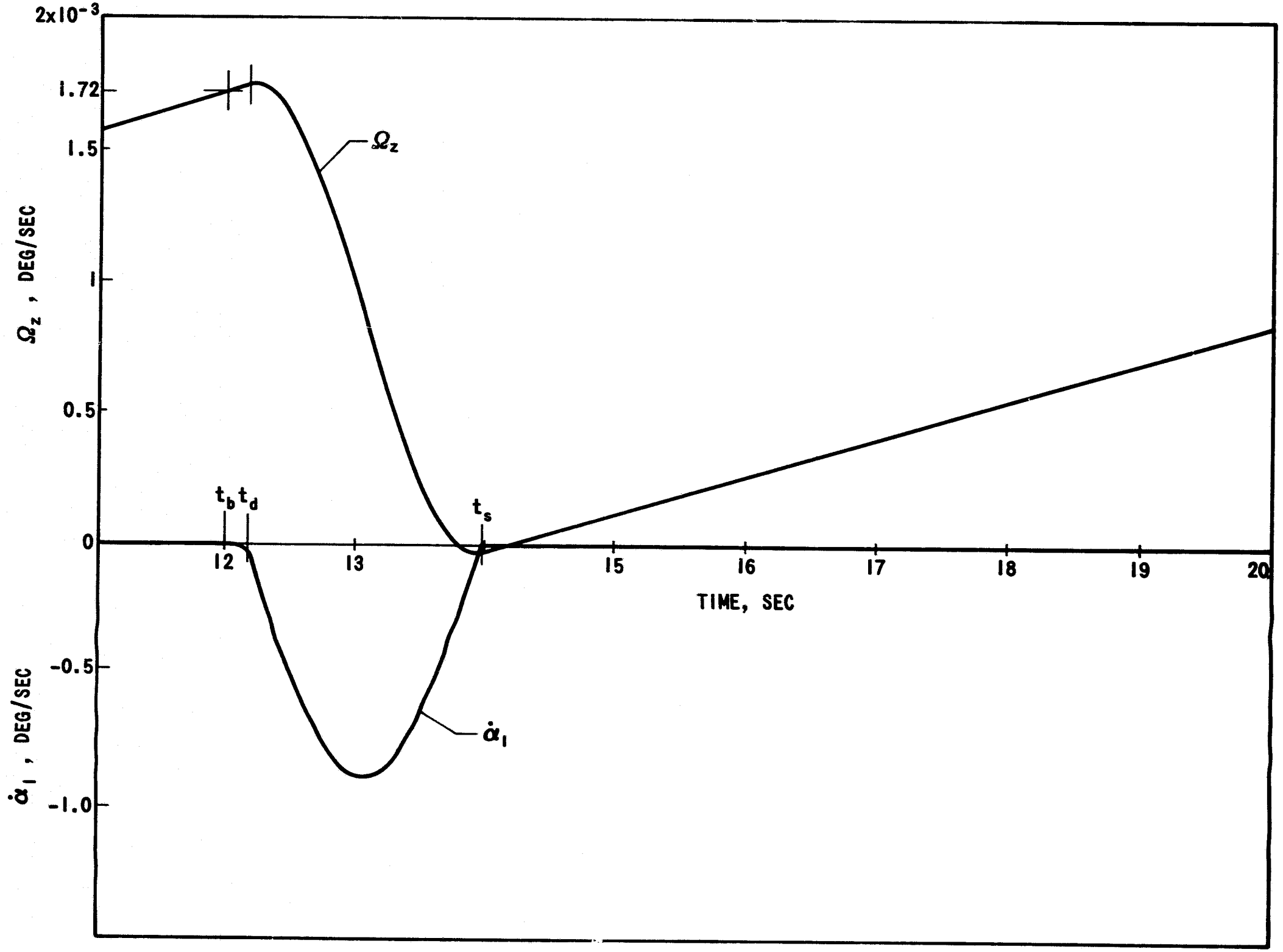

FIGURE 12 - COULOMB FRICTION DROP AT $\dot{\alpha}_1$ = -0.0034 DEG/SEC. B_σ = 0.03 FT.LB. ANGULAR VELOCITIES Ω_z AND $\dot{\alpha}_1$ AS FUNCTIONS OF TIME

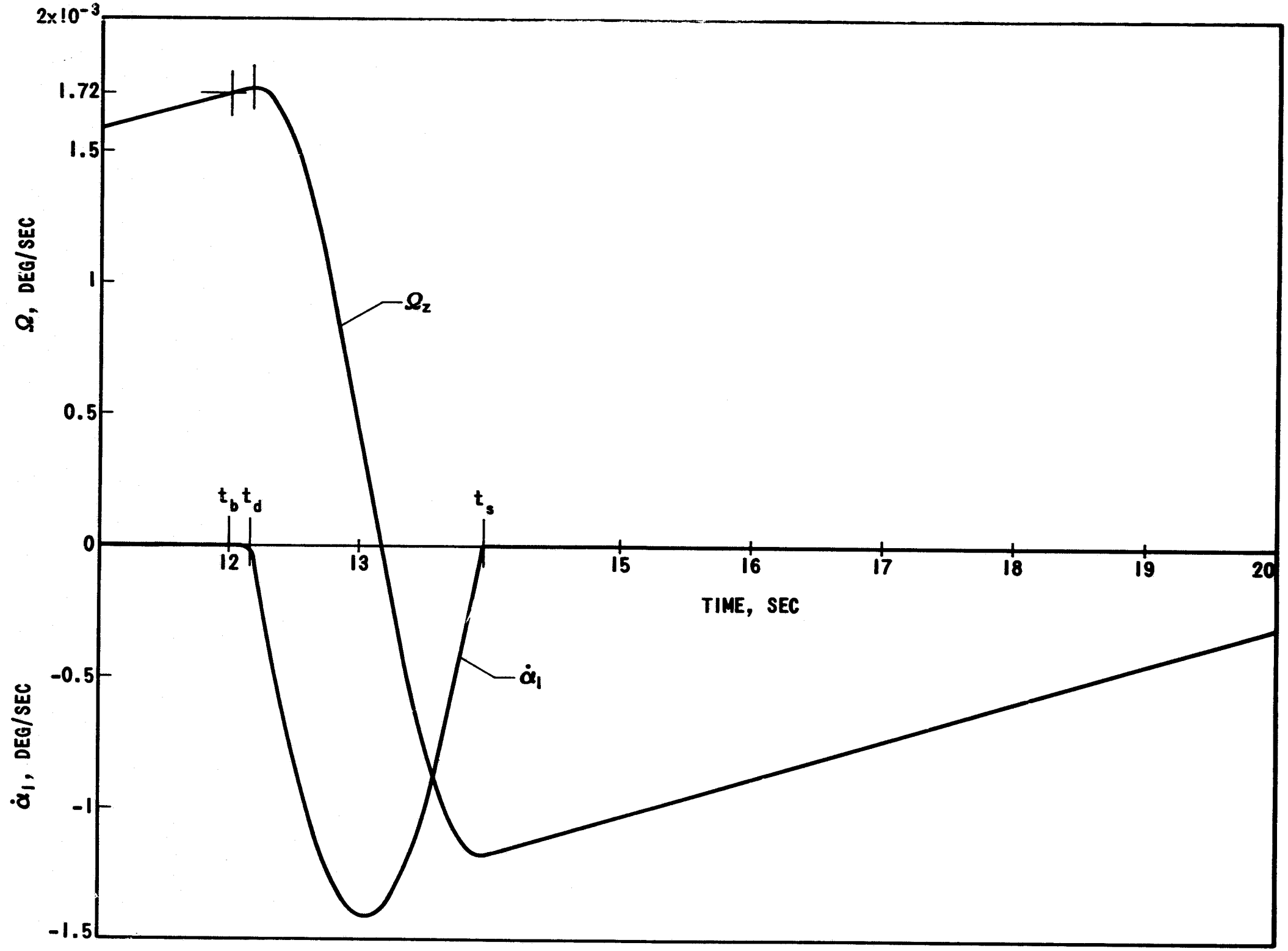

FIGURE 13 - COULOMB FRICTION DROP AT $\dot{\alpha}_I$ = -0.0034 DEG/SEC. B_σ = 0.01 FT.LB. ANGULAR VELOCITIES Ω_z AND $\dot{\alpha}_I$ AS FUNCTIONS OF TIME

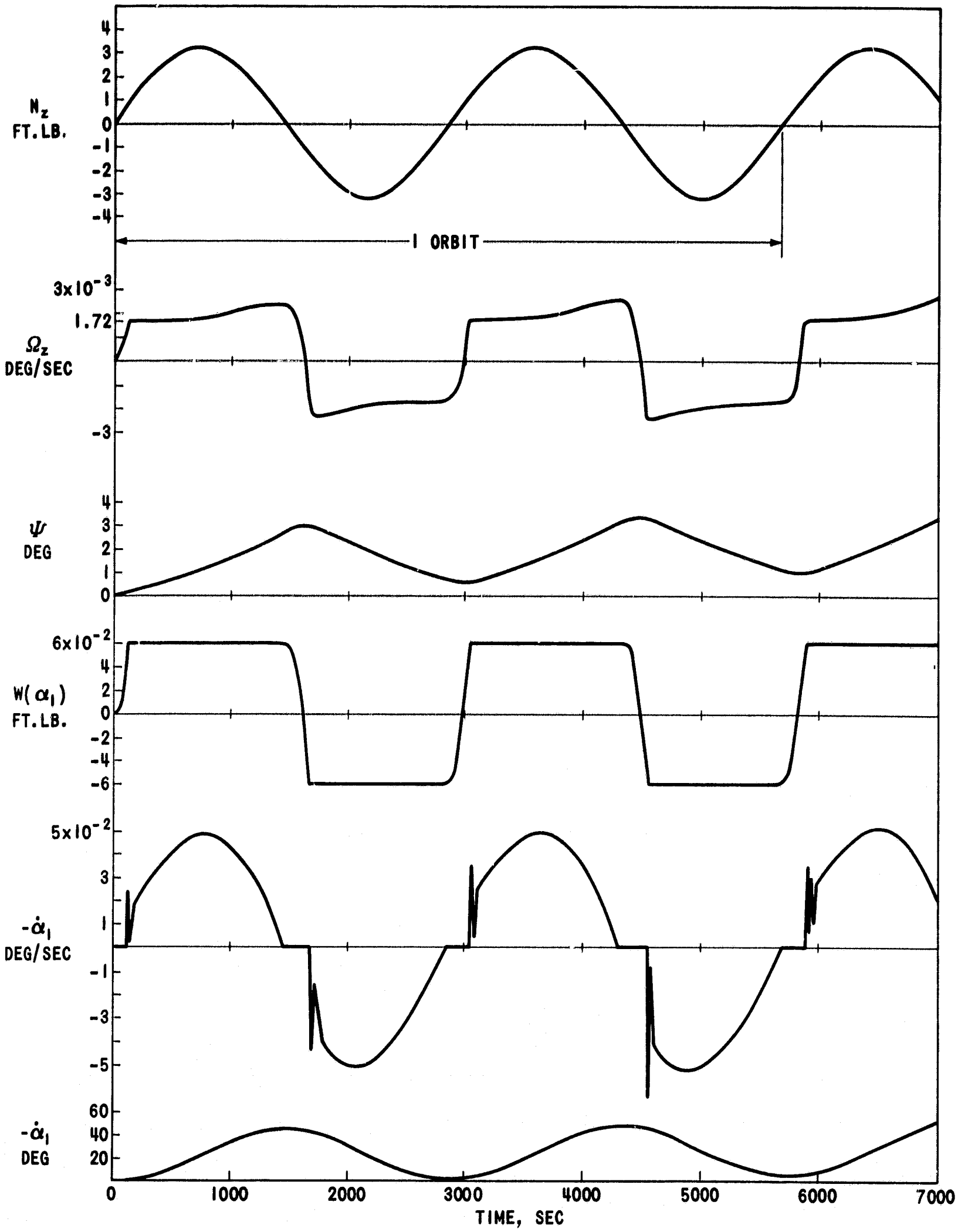

FIGURE 14 - EXTERNAL TORQUE IS SINUSOIDAL FUNCTION. NO COULOMB FRICTION DROP. EXTERNAL TORQUE N_z, TORQUE $W(\alpha_1)$, ANGULAR VELOCITIES Ω_z AND $\dot{\alpha}_1$, AND ANGLE Ψ AS FUNCTIONS OF TIME.